Journal of GeoEngineering, Vol. 9, No. 2, pp. 75-83, August 2014
http://dx.doi.org/10.6310/jog.2014.9(2).3

EFFECTS OF MULTIPLE CORRECTIONS ON TRIAXIAL COMPRESSION TESTING OF SANDS

Tarek Omar [1] and Abouzar Sadrekarimi [2]

ABSTRACT

Triaxial tests are often used to determine the behavior and strength characteristics of soils for geotechnical engineering analysis and design. Triaxial testing involves many sources of error that could significantly affect shear strength parameters if not corrected. These errors and the available correction methods are thoroughly reviewed in this study in a series of monotonic triaxial compression tests on loose Ottawa sand specimens. The significance of each correction on the triaxial test results and the achieved adjustments of the shear strength parameters and void ratio are discussed and evaluated. It is found that negligence in making corrections accounting for these errors could result in an overestimation of as much as 44% and 14.7° in the measurement of undrained and drained shear strength parameters, respectively.

Key words: Granular materials, geotechnical engineering, strength and testing of materials.

1. INTRODUCTION

Laboratory shear tests conducted to understand soil behavior have been improved with the continuous advent of advanced testing devices. Triaxial tests on cylindrical specimens are often used for measuring the shear behavior of soils. The most significant errors associated with triaxial testing of soils are the variation of specimen cross-sectional area during shearing, and the volume change due to back-pressure saturation or membrane penetration resulting from the variation of the effective confining stress. In addition, the bedding effect from using layers of latex sheets in enlarged and lubricated end platens technique could cause error in the measured axial deformation. The membranes' resistance to the applied axial and radial stresses may also influence the measured shear strength.

In this study, monotonic triaxial compression tests are performed on loose Ottawa sand specimens to determine the volumetric response and shear behavior of the specimens at large strains where a critical state is produced. Specially-designed moulds and platens are used to reduce end restraint effects and improve specimens' uniform deformation. Corrections are made to account for the volume change due to back pressure saturation (ASTM D4767, 2011) and membrane penetration (Baldi and Nova 1984), axial deformation due to bedding error (Sarsby *et al*. 1980), stress correction due to membrane resistance (ASTM D7181, 2011), and the change of specimen cross-sectional area during shear (Garga and Zhang 1997). The significance of each correction on the triaxial test results and the achieved adjustments of the shear strength parameters and void ratio are subsequently discussed and evaluated.

Manuscript received April 23, 2014; revised June 24, 2014; accepted July 8, 2014.
[1] Ph.D. candidate (corresponding author), Department of Civil and Environmental Engineering, Western University, London, Ontario, Canada (e-mail: tomar3@uwo.ca).
[2] Assistant Professor, Department of Civil and Environmental Engineering, Western University, London, Ontario, Canada.

2. EXPERIMENTAL PROGRAM

2.1 Triaxial Compression Testing System

The triaxial tests of this research were conducted using an automated stress path triaxial compression testing system (SIGMA-1^{TM} 5K model) manufactured by GeoTac, Texas, USA. The main components of this apparatus include a triaxial cell, a loading frame, two electromechanical pressure pumps, and a data acquisition and control system. The system also includes an external load cell, a deformation sensor, and three fluid pressure sensors. Figure 1 provides a schematic diagram of this system.

The axial load is applied by the loading frame in displacement-control (up to a rate of 25.4 mm/minute) or load-control (up to a maximum axial load of 10,000 N) modes. Soil resistance to the axial load is measured by a 2,000 N external load cell attached to the loading frame. All tests of this study were conducted using the displacement-control mode at a rate of 5%/hour. The axial deformation of the sample during shear was measured externally by a linear variable displacement transducer (LVDT) on the loading piston of the triaxial cell. Two electromechanical pumps (*i.e.* cell and pore pressure pumps) were used to control and measure the volume and pressure of the cell fluid and specimen's pore water. All sensors were calibrated at the commencement of the testing program.

2.2 Properties of the Tested Sand and Specimen Preparation Method

A clean, uniformly-graded Ottawa sand – classified as a SP according to the Unified Soil Classification System (ASTM D2487, 2011) – with round to sub-round particle shapes is used in the tests of this study. Sieve analysis was performed on the sand, and average mean particle size (D_{50}), coefficient of uniformity (C_U), and coefficient of curvature (C_C) of 0.22 mm, 1.71, and 1.07 were determined, respectively. Specific gravity of the sand particles (G_S), and maximum and minimum void ratios of

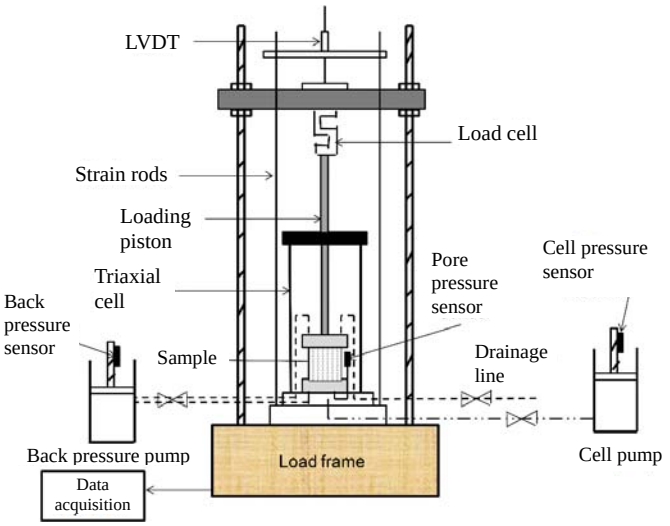

Fig. 1 Schematic diagram of the triaxial testing system

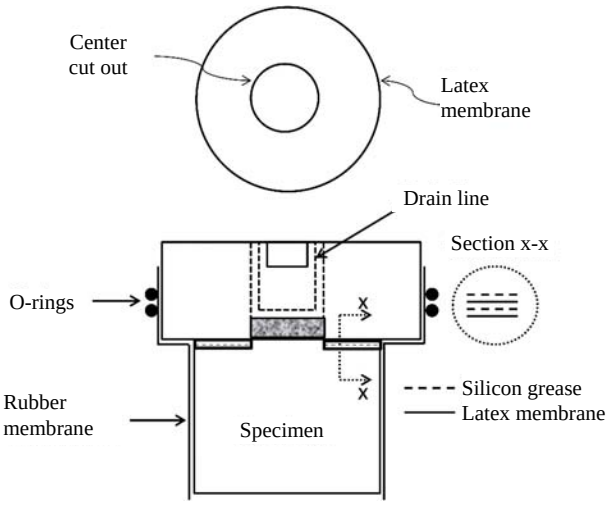

Fig. 2 Procedure of developing lubricated end platens

respectively 2.65, 0.821, and 0.487 were measured following the ASTM standard procedures. Since the purpose of this study was to investigate the influence of different errors and multiple corrections on the testing of loose sands, all specimens were prepared by moist tamping. In this method, the surface tension among moist sand particles allows the creation of very loose sand fabrics even at void ratios greater than the maximum void ratio of a dry sand obtained from the ASTM D4253 (2006) procedure. Cylindrical sand specimens were prepared with nominal diameters (D_s) of 38, 50, and 70 mm and height (H_s) to D_s ratios of unity to reduce non-uniformity at larger strains. As illustrated in Fig. 2, two latex membranes of the same specimen diameter and with 0.3 mm thicknesses were smeared with a thin layer of silicon grease and placed over specimen caps in order to reduce specimen end effects. In order to minimize void ratio non-uniformities within the specimens, the under compaction technique introduced by Ladd (1978) was employed to achieve a relatively uniform density throughout the specimen height. A small vacuum (about 4 to 5 kPa) was subsequently applied by the pore pressure pump in order to provide temporary confinement and hold the specimen in place during dismantling of the mould while the actual specimen height (H_o) and diameter were measured in order to determine its initial volume (V_o) and thus initial void ratio (e_o). The cylindrical triaxial cell was then assembled and placed in the load frame, filled with de-aired water, and the vacuum pressure was replaced by an external cell pressure of 10 kPa. The initial vacuum pressure was necessary to maintain the specimen shape before the application of the external cell pressure, otherwise the specimen collapsed upon the removal of the specimen mould. As complete saturation of the specimen was required to ensure accurate volume change and pore pressure measurement, carbon dioxide (CO_2) was first percolated through the specimens followed by flushing with water. The saturation procedure was proceeding with a backpressure saturation phase as recommended by Black and Lee (1973) until a pore water pressure parameter, B of at least 0.97 was achieved in all specimens.

2.3 Consolidation and Shearing

Isotropic consolidation commenced after the completion of specimen saturation by increasing the confining pressure to the target isotropic consolidation stress (p'_c) while recording specimen volume change for calculating consolidation void ratio (e_c) and relative density (D_{rc}). The specimens were sheared following isotropic consolidation. During shear the total cell pressure was kept constant while advancing the axial loading piston on the specimen cap at a constant strain rate of 5%/hour up to an axial strain of 30%. The shear strain rate was chosen based on ASTM D4767 (2011) and ASTM D7181 (2011) guidelines to ensure pore pressure equalization during undrained shearing and complete excess pore pressure dissipation during drained shear. Table 1 summarizes the specifications of the triaxial tests conducted in this study.

Table 1 Specifications of the triaxial compression tests

Test No.[a]	D_s (mm)	p'_c (kPa)	e_c	D_{rc} (%)
MT-1D	70	500	0.771	15
MT-2D		300	0.779	13
MT-3D		200	0.785	11
MT-4D		100	0.797	7
MT-5UD		500	0.775	14
MT-6UD		300	0.782	12
MT-7UD		200	0.791	9
MT-8UD		100	0.797	7
MT-9D	50	500	0.761	18
MT-10D		300	0.769	16
MT-11D		200	0.773	14
MT-12D		100	0.786	10
MT-13UD		500	0.769	16
MT-14UD		300	0.775	14
MT-15UD		200	0.785	11
MT-16UD		100	0.795	8
MT-17D	38	500	0.76	18
MT-18D		300	0.766	16
MT-19D		200	0.775	14
MT-20D		100	0.786	10
MT-21UD		500	0.766	16
MT-22UD		300	0.773	14
MT-23UD		200	0.784	11
MT-24UD		100	0.794	8

[a] D and UD in test labels indicate drained and undrained shearing, respectively.

3. CORRECTIONS FOR TRIAXIAL COMPRESSION TESTS

Triaxial shear tests involve several sources of errors that could be significant in interpreting test results if uncorrected. The methods to account for these errors and the applied corrections along with the obtained results are described in the following paragraphs.

3.1 Correction for Volume Change during Saturation

In conventional triaxial tests, e_c is calculated based on the initial specimen dimensions taken before assembling the cell and the void ratio changes occurring during backpressure saturation and consolidation. The correct assessment of this void ratio is particularly important in the critical state testing of loose sands because of the higher sensitivity of the critical state line to void ratio variations. The sample volume changes during flushing and backpressure saturation can be estimated by the volume change of the cell fluid or by measuring the axial and radial deformations of the specimen using specialized sensors. Imaging techniques using either a high resolution camera or a three-dimensional laser scanner are also utilized in some studies.

As described earlier, saturation of the moist tamped specimens in this study was accomplished by flushing the samples with CO_2 followed by de-aired water, and then applying backpressure. Since the purpose of this study was to investigate the effects of measuring errors and corrections on loose sands and critical state testing, all specimens were prepared at e_o = 0.821, corresponding to a relative density of 0%. Volume changes occurring during backpressure saturation were estimated by measuring the axial strain (ε_a) of the specimen while making contact between the axial loading shaft and the specimen top cap after saturation, and calculating the radial strain (ε_r) and thus the volumetric strain (ε_v) of the specimen from its Poisson's ratio ($\nu = -\varepsilon_r / \varepsilon_a$). This procedure is described by the following relationships:

$$\varepsilon_v = \varepsilon_a + 2\varepsilon_r = (1-2\nu)\,\varepsilon_a \tag{1}$$

$$\Delta V_s = \varepsilon_v V_o = (1-2\nu)\,\varepsilon_a\, V_o = (1-2\nu)\,\Delta H_s A_o \tag{2}$$

where A_o is the initial cross sectional area of the specimen, and ΔH_s is the specimen's height change during saturation. An average Poisson's ratio of 0.34 was obtained for all specimens from specimen deformations measured during isotropic consolidation.

The calculated ΔV_s indicated that void ratio decreased by an average of 1.1% (0.008 – 0.01) following back-pressure saturation which corresponds to about 2.4% to 3.0% in terms of relative density changes. Accordingly, neglecting saturation volume changes could lead to an overestimation of the specimens' void ratio and eventually an incorrect critical state line. This could further lead to about 2 ~ 3% underestimation of the undrained critical strength of the soil, $s_{u(\text{critical})}$ or effective friction angle (ϕ'_{cs}) resulting from the inaccurate cross-sectional area of the specimen before shear.

3.2 Correction for Volume Change due to Membrane Penetration

In triaxial tests on granular soils, volume change due to membrane penetration occurs when the latex membrane penetrates into the surface irregularities of the specimen with increasing of the effective minor principal stress (σ'_3), while the membrane tends to return to its original position when σ'_3 is reduced. The amount of the resulting volume change is equal to the difference between the total volume of water driven out of the sample and the actual volume change of the soil skeleton. This phenomenon was first recognized by Newland and Alley (1957) and since then it has been of considerable interest for many researchers (Raju and Sadasivan 1974; Baldi and Nova 1984; Nicholson *et al.* 1993; Ansal and Erken 1996; Zhang 1997; Sivathayalan and Vaid 1998). In a drained triaxial test, σ'_3 remains constant and thus membrane penetration is negligible, whereas in an undrained triaxial shear test σ'_3 could change substantially as a result of shear-induced pore water pressure. The amount of membrane penetration is a function of many factors including σ'_3, grain size, grain shape, gradation, density of the sample, the surface area of the sample in contact with the rubber membrane, and the characteristics of the rubber membrane such as its thickness and extension modulus (Raju and Sadasivan 1974).

Several methods are developed to account for the volume changes due to membrane penetration (ΔV_m). For example, Baldi and Nova (1984) investigated the membrane penetration in triaxial tests and found that ΔV_m depended strongly on D_{50}, σ'_3, and the diameter of the specimen (D_s) as well as the membrane characteristics. Based on their analysis, a quantitative correction was developed to account for membrane penetration in a typical triaxial test as below:

$$\Delta V_m = \left(\frac{D_{50}}{2\times D_s}\right)\times\left[V_o \times\left\{\frac{\sigma'_3 \times D_{50}}{E_m \times t_m}\right\}\right]^{\frac{1}{3}} \tag{3}$$

where E_m is the Young's modulus of the membrane material, and t_m is the thickness of the membrane. According to Eq. (3), the amount of ΔV_m in an undrained test mainly depends on σ'_3, with a higher σ'_3 producing larger membrane penetration. Nicholson *et al.* (1993) found that the influence of sample density on membrane penetration was relatively small in comparison to the influence of D_{50}. Zhang (1997) studied the effect of membrane thickness on the amount of membrane penetration for two sands with different initial relative densities and found that membrane thickness significantly affected the amount of penetration in both sands. The thinner the membrane the higher the volume change was due to membrane penetration. The amount of membrane penetration in this study is calculated using Eq. (3) as it accounts for most of the factors that affect membrane penetration. Correction for membrane penetration during isotropic consolidation was considered in all of the tests performed in this study by correcting the recorded volume change after consolidation and accordingly e_c. D_{50} of the tested sand, t_m, and E_m of the rubber membrane were measured respectively as 0.22 mm, 0.3 mm, and 1,350 kPa. The change in e_c due to membrane penetration was insignificant with an average of 0.36% (0.002 ~ 0.003), corresponding to about 0.6 to 0.9% changes in D_{rc}. This can be attributed to the fine gradation of the tested sand that limited the

amount of membrane penetration into the surface irregularities of the specimen. During undrained shearing, specimen volume was kept constant throughout shearing by closing all the drainage lines. On the other side, the increase in shear-induced excess pore water pressure pushed the membrane out of the voids (or into the voids if the excess pore water pressure had decreased). This depends on the water modulus which is greatly affected by the degree of specimen saturation and therefore the actual effect of membrane penetration on pore water pressure generation was insignificant due to the slightly incomplete saturation (*e.g.*, S_r < 100%, $B = 0.97$). Note that the effect of membrane penetration on pore pressure response merely inhibits perfectly undrained shearing and it is not a measuring error as the actual shear- induced pore water pressure is continuously measured throughout the experiment.

3.3 Effects of Specimen Boundaries

A sand specimen will ideally deform as a right circular cylinder throughout a triaxial compression shear test with no boundary restraints, but it often exhibits bulging deformation as a result of friction at the specimen ends (Bishop and Green 1965). Specimen bulging produces non-uniform stresses and strains in a triaxial specimen which could significantly affect the measured strength, strain-softening, pore pressure or volume change behavior of a soil specimen particularly at large deformations associated with critical states. Different methods have been pursued to reduce the effect of specimen boundaries, but the lubricated end platens technique developed by Rowe and Barden (1964) has been the most effective method (Zhang 1997).

Enlarged and lubricated end platens were employed in the experimental work of this study to allow free radial expansion of the specimen and minimize the bulging deformation of the specimens during shear. Enlarged end platens were designed to accommodate the radial expansion of the specimen at shear strains of up to 30%. As illustrated in Fig. 2, the lubricated ends consisted of two sheets of 0.3 mm thick rubber discs which were separated with a thin layer of high vacuum silicone grease. The rubber discs were cut to the specimen diameter with a central hole cut to the diameter of the porous stone to allow drainage. An additional layer of high vacuum silicon grease was smeared on the rubber discs in order to provide a smooth and frictionless sliding on the end platens. The slenderness or the height to diameter (H_s/D_s) ratio of a specimen is another factor that affects the bulging deformation. Bishop and Green (1965) illustrate that specimens with $H_s/D_s = 1$ and lubricated ends could deform nearly uniformly during drained shear, while more slender specimens ($H_s/D_s = 2$) displayed a bulging deformation irrespective of end restraints. Significant specimen bulging was observed at large shear strains in trial tests of this study on specimens with $H_s/D_s = 2$, regardless of whether the specimen ends were enlarged and lubricated or not. Therefore, it was decided to adopt a slenderness ratio of unity along with lubricated and enlarged end platens to minimize the effects of specimen end restraint and allow for uniform specimen deformation and homogeneous stress distribution throughout the triaxial shear tests. This is particularly necessary for critical state testing which requires shearing to large shear strains. Accordingly, specially designed split moulds were constructed and used for preparing specimens that would accommodate enlarged platens. As a result, specimen bulging was significantly reduced resulting in more homogeneous specimen deformations, although it never completely disappeared. Subsequently, a comprehensive experimental investigation was made to further minimize specimen bulging. It was determined that rigid stainless steel platens would further reduce bulging by preventing the microscopic penetration of sand particles into the end platens (which would produce additional end friction). The regular acrylic platens were subsequently replaced with hardened stainless steel end platens. Figure 3 demonstrates the effectiveness of lubricated ends in producing a uniform specimen deformation pattern at an axial strain of 30% in the triaxial tests of this study.

A series of pilot tests were conducted on 50 mm specimens without lubricated platens and the results were compared with the production experiments in order to quantify the improvements gained by enlarging and lubricating the platens at large axial strains. Two undrained triaxial compression tests were performed for each case at $p'_c = 100$ kPa and 300 kPa corresponding to $D_{rc} =$ 8% and 14%, respectively. The stress-strain responses and the mobilized friction angles (ϕ'_{mob}) are compared in Fig. 4. According to this figure, the final deviator stress (q) and ϕ'_{mob} reduced by an average of 13% and 2° with the employment of enlarged and lubricated end platens. This reduction occurs as friction at specimen boundaries is reduced which leads to more uniform specimen deformation and stress distribution within the specimen. We also observed that the shear-induced excess pore pressure was slightly increased with lubricated ends, further reducing the undrained deviator stress. Accordingly, an average overestimation of about 10% in the measurement of undrained critical strength, $s_{u(\text{critical})}$ was calculated if the platens were not lubricated. These results are further supported by those observed by some other investigators (Olson and Campbell 1964; Ueng *et al*. 1988).

3.4 Area Correction for Specimen Deformation

The axial stress is computed by dividing the axial force by the cross-sectional area of the specimen. Ideally, the cross-sectional area is calculated based on the assumption that the sample deforms as a right circular cylinder during shear. As it is necessary to shear sand samples to large axial strains for critical state testing, initially-cylindrical specimen deforms substantially during the test and may significantly bulge. This bulging deformation makes the calculation of the cross-sectional area difficult and results in errors in the calculated deviator stress and accordingly the critical strength of the sand. Therefore, it is necessary to consider an effective cross-sectional area that takes into account the bulged shape of the specimen with a proper deformation pattern. Several methods have been developed for calculating the effective cross sectional area (A_e) of a specimen during shear. The choice of the area correction method should be based on the observed deformation profile of the specimen during and after shear. In the cylindrical deformation correction method recommended by the ASTM standard testing method D4767 (2011), the specimen is assumed to deform as a right cylinder during shear (La Rochelle *et al*. 1988). The corrected area is calculated as $A_e = A_c (1 - \varepsilon_v) / (1 - \varepsilon_a)$ where A_c is specimen's cross-sectional area before shearing, and ε_v and ε_a are the volumetric and axial

(a) (b)

Fig. 3 Deformation pattern of a loose sand specimen (a) without, and (b) with enlarged and lubricated end platens in triaxial compression tests at 30% axial strain

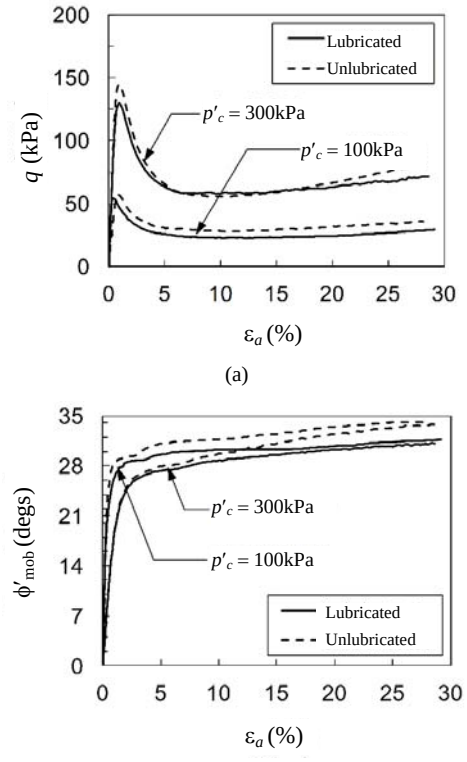

Fig. 4 Effect of lubricated end platens on (a) undrained deviator stress – axial strain, and (b) mobilized friction angle (ϕ'_{mob}) in triaxial compression tests on 50 mm specimens

strains, respectively. At a more complex level, the specimen is assumed to deform as a parabola (similar to a barrel) and A_e is computed at the mid-height of the specimen as $A_e = A_c\left[-0.25+\sqrt{(25-20\varepsilon_a-5\varepsilon_a^2)}/4(1-\varepsilon_a)\right]^2$. Zhang and Garga (1997) also developed a method to correct the cross-sectional area of triaxial specimens. They performed triaxial tests where the samples' diameters were physically measured with a caliper at different strain levels and the deformation profile of the specimen was determined in each test. They found that the maximum specimen diameter occurred at the mid-height of the specimen and the specimen diameter changes with height at different axial strains were parabolic. Therefore, they suggested using the average specimen diameter within the middle third portion of the sample ($D_{1/3}$) to calculate the deviator stress as:

$$D_{1/3} = D_{\max} - \frac{1}{12}(D_{\max} - D_c) \tag{4}$$

$$D_{\max} = \frac{D_c}{4}\left[\left\{30\frac{(1-\varepsilon_v)}{(1-\varepsilon_a)}-5\right\}\right]^{\frac{1}{2}} - 1 \tag{5}$$

As illustrated in Fig. 3, the lubricated end platens reduced but did not eliminate specimen bulging as the specimens exhibited a slightly parabolic shape at the end of the tests. Accordingly, the method developed by Zhang and Garga (1997) for a parabolic specimen deformation is adopted to account for the enlarged area of the specimen. Note that the area correction method recommended by the ASTM standard D4767 (2011) assumes that the specimen deforms as a right circular cylinder. A right cylindrical deformation would occur if the specimen ends were perfectly frictionless and this correction could be used to replicate stress-strain response of an ideal specimen with no boundary effects. Figure 5 compares the undrained stress-strain responses and mobilized friction angles (ϕ'_{mob}) of loose sand specimens obtained using these area correction methods at p'_c = 100 kPa.

Compared to the final deviator stress without any area correction, the cylindrical (ASTM D4767, 2011), and the parabolic (Zhang and Garga 1997) area correction methods have reduced the final deviator stresses by an average of 30% and 24%, respectively. The corresponding friction angles (ϕ'_{cs}) are also decreased by up to 7° and 5°. The differences in the amounts of deviator stress and ϕ'_{mob} reductions from the two area correction methods further supports that the lubricated platens reduced but did not completely eliminate end friction. As shown in Fig. 5, these differences become significant at the end of the test and they can lead to the overestimation of drained (ϕ'_{cs}) and undrained ($s_{u(critical)}$) shear strengths if the actual deformation pattern of the specimen is not taken into account in selecting the appropriate method of area correction. This error would further increase if lubricated end platens were not employed.

3.5 Correction for Bedding Error

A uniform specimen deformation was nearly achieved by using enlarged and lubricated end platens with specimens that had a height to diameter ratio of one. Although the use of lubricated latex sheets at the top and bottom of the specimens provided significant reduction in end restraint, they produced additional bedding errors with the application of the axial load as the latex sheets compressed and penetrated into the cavities among the sand particles. This phenomenon directly affected the precise measurement of ε_a. Sarsby *et al.* (1980) studied the compression of rubber layers in triaxial tests and the importance of correcting the measured axial displacement for the compression of latex sheets. They found that the bedding error was a logarithmic function of the effective axial stress, σ'_1. Russell and Khalili (2004) subsequently conducted a series of one-dimensional compression tests on sands with and without lubricated latex layers and found that the compression of a single layer of rubber (Δ) was a logarithmic function of σ'_1 as shown in the following equation:

$$\Delta\,(\text{mm}) = 0.0352 \ln \sigma'_1(\text{kPa}) - 0.0713 \tag{6}$$

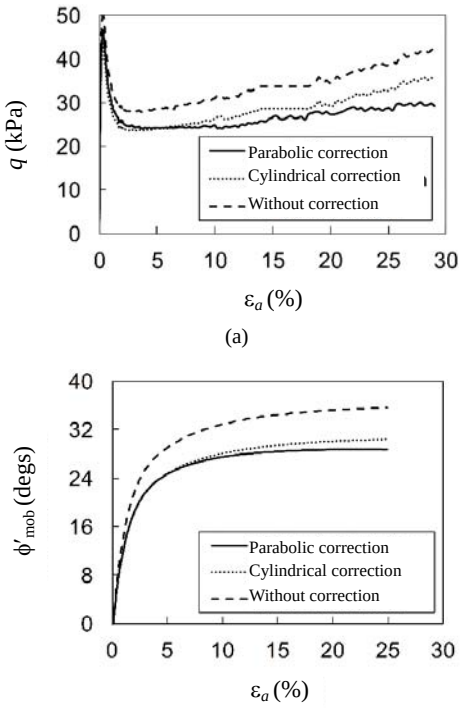

Fig. 5 Effect of area correction on (a) undrained stress- strain response and (b) mobilized friction angle (ϕ'_{mob}) of loose sand in triaxial compression tests on 50 mm specimen diameters at p'_c = 100 kPa

To improve the accuracy of axial displacement measurement during shear in the triaxial tests of this study, the bedding effect of 4 latex sheets (two on each end of a specimen) is accounted for by deducting their compression from the measured axial displacement. Equation (6) is employed to estimate the amount of latex compression resulting from the axial stress applied on the specimen. Note that as the rubber membrane was already compressed following the consolidation stage, it was necessary to also include the amount of rubber compression produced by p'_c. The bedding error, if neglected, could greatly affect the measured ε_a and lead to significant underestimation of shear modulus from triaxial testing results. Our analysis indicated that the bedding error increased with increasing p'_c and it was larger in drained shear tests due to the steady increase of σ'_1. The maximum bedding deformation in the experiments in this study was calculated as 0.38 mm, corresponding to about 5.1% of the measured total axial displacement.

3.6 Correction for Membrane Resistance

The rubber membrane used to seal a specimen in triaxial testing can carry a portion of the load applied on the specimen. This could be particularly significant in measuring the reduced $s_{u(\text{critical})}$ of loose soils after strain-softening and liquefaction. The ASTM standard method D7181 (2011) provides a correction for membrane resistance and recommends its application for when the effect of membrane resistance on deviator stress is greater than 5%. According to ASTM D7181 (2011), the shear stress carried by the membrane Δq_m (kPa) is calculated by the following equation:

$$\Delta q = 4\frac{E_m\, t_m\, \varepsilon_a}{D_c} \tag{7}$$

where E_m (kPa) is the Young's modulus of the membrane material, t_m (mm) is the thickness of the membrane, and D_c (mm) is the specimen diameter after consolidation. Correction for membrane resistance was applied according to the ASTM standard method D7181 (2011) for all the experiments performed in this study. For accurate estimation of membrane resistance, the Young's modulus of the latex membrane material was determined from an extension test according to the ASTM D7181-11 standard procedure. The test involved stretching a one inch wide loop of the membrane with weights and measuring the force per axial deformation of the membrane. A modulus (E_m) of about 1,350 kPa was obtained. Figure 6 shows the influence of membrane resistance on the stress-strain responses of 38 mm loose sand specimens at p'_c = 100 kPa. As shown in Fig. 6, the contribution of membrane resistance increases with increasing axial strain and particularly at large strains where the reduced $s_{u(\text{critical})}$ is mobilized in a loose sand. Neglecting this correction could lead to an overestimation of up to 8% in the measured critical strength. For example, $s_{u(\text{critical})}$ = 19.9 kPa was measured in the 38 mm specimen at p'_c = 100 kPa, which includes the additional resistance of 3.0 kPa ($\approx 0.15 s_{u(\text{critical})}$) provided by the membrane. Therefore, membrane resistance should be considered for accurate evaluation of deviator stresses particularly at the critical state.

4. PRACTICAL IMPLICATIONS FOR LABORATORY TRIAXIAL TESTING

The errors associated with triaxial testing and the correction techniques employed for each error were briefly reviewed above. It was observed that the difference between the corrected and uncorrected data generally increased with increasing ε_a. Figure 7 demonstrates the relative effect of each correction on the effective stress paths and ϕ'_{cs} for the 50 mm specimens at p'_c = 100 kPa and 300 kPa. These plots clearly show the comparatively significant effect of area correction in reducing the mobilized deviator stress and ϕ'_{cs}.

In order to assess the significance of each error, identify how the corrections interact and compare the importance of the corrections, the aforementioned errors and the applied correction methods as well as the percentages of improvement of the associated parameter are summarized in Table 2 based on the triaxial tests of this study. The data in Table 2 show that specimen bulging deformation is the most significant source of error affecting $s_{u(\text{critical})}$ and ϕ'_{cs}, followed by the effect of membrane resistance and end restraint. While bulging deformation and end restraint errors were largely corrected by the area correction and the using of enlarged and lubricated end platens in this study, specimen end restraints have an unsafe effect on triaxial test results by increasing soil shear strength and friction angle. According to Table 2, the studied parameters ($s_{u(\text{critical})}$, ϕ'_{cs}, $e_{critical}$) are affected by multiple sources of error, and $s_{u(\text{critical})}$, ϕ'_{cs}, and $e_{critical}$ could be overestimated up to 44%, 14.7° and 0.7%, respectively if no correction is applied. From the above analysis, correcting for the specimen cross-sectional area is the most significant correction for $s_{u(\text{critical})}$ and ϕ'_{cs} which needs to be adopted based on the observation of specimen shearing deformation. Accounting for these corrections is particularly necessary in critical state testing and liquefaction studies of loose sands and for the determination of the critical state line which is very sensitive to void ratio variations.

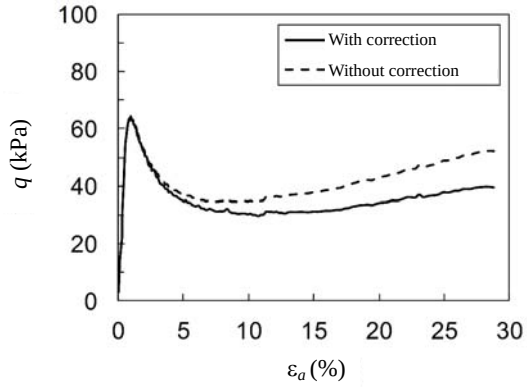

Fig. 6 Effect of membrane resistance on the stress- strain responses of undrained triaxial compression tests on 38 mm diameter loose sand specimens at p'_c = 100 kPa

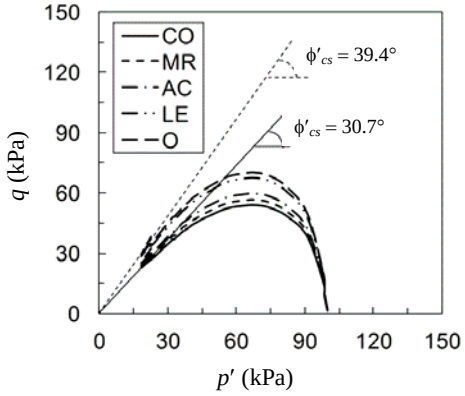

(a)

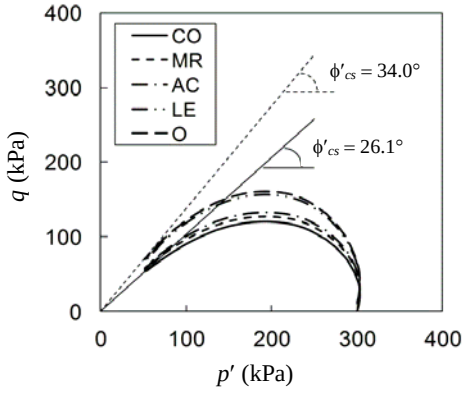

(b)

Fig. 7 Effect of multiple corrections on effective stress paths and ϕ'_{cs} from the undrained triaxial tests on 50 mm diameter specimens at (a) p'_c = 100 kPa, and (b) p'_c = 300 kPa (O: original data without any corrections; LE: with lubricated and enlarged platens; AC: with area correction; MR: with correction for membrane resistance; CO: with all corrections)

Table 2 Summary of the applied corrections and percentage improvements of triaxial test results on loose Ottawa sand

Correction	Parameter	Mechanism	Adjustment
Enlarged and lubricated platens	$s_{u\ (critical)}$	End restraints	–10% (–8 to –12)
	ϕ'_{cs}		–3.6° (–3.1° to –4.2°)
Area correction	$s_{u\ (critical)}$	Specimen bulging	–24.5% (–20 to –29)
	ϕ'_{cs}		–8.9° (–7.8° to –10°)
Membrane resistance	$s_{u\ (critical)}$	Membrane resistance	–11% (–8 to –15)
	ϕ'_{cs}		–3.1° (–2.6° to –3.6°)
Volume change	$s_{u\ (critical)}$	Saturation	1.5% (2.0 to 3.0)
	ϕ'_{cs}		0.9° (0.8 to 1.0)
	$e_{critical}$		–1.1% (–0.9 to –1.3)
	$e_{critical}$	Membrane penetration	0.36% (0.32 to 0.40)
Bedding error	ε_a	Latex compression	–2.5% (–0.5 to –5.5)

5. CONCLUSIONS

The experimental errors affecting the triaxial shearing behavior of loose sand have been thoroughly reviewed in this study, which illustrated the significant effects of end restraint and triaxial data corrections on sand shearing behavior. Non-uniform deformations at large strains (which is often required to achieve a critical state), significantly affect the strength of sands. It was demonstrated that lubricated and enlarged end platens are helpful methods to minimize the effects of end restraint and promote uniform deformations during shear. As a result of these improvements, accurate volume change in drained shear tests as well as lower deviator stresses and higher pore pressures were measured in the undrained shear tests. It was found that non-lubricated end platens could result in an average of 10% overestimation of $s_{u(critical)}$. While lubrication improved the uniformity of the specimens' deformation, it did not completely eliminate non-uniform deformations and the final specimen shapes were slightly parabolic and thus an area correction conforming to the shape of the deformed specimens was applied to account for this barreling deformation of the specimen and correct the calculated axial stress. Accordingly, the critical strength was further reduced by an average of 24.5%. The bedding error due to the compression of the latex membrane used in the enlarged platens technique increased the measured axial strain by an average of 2.5%. It was further observed that neglecting membrane resistance could lead to the overestimation of sand strength up to an average

of 11%. An important factor affecting the behavior of sands is its void ratio. The volume change during back pressure saturation and due to membrane penetration could affect the determination of soil void ratio. The results of volume change analyses of this study indicated that ignoring the volume change during saturation could lead to an overestimation of the specimen's void ratio up to 0.01 which corresponds to about 3% in terms of relative density. It was found that area correction was the most significant source of error observed in this comprehensive study which requires appropriate correction for triaxial shear testing of loose sands.

LIST OF NOTATIONS

Δ = compression of a rubber membrane layer
ΔH_s = change of specimen height during saturation
Δq_m = membrane resistance
ΔV_m = specimen volume change due to membrane penetration
ΔV_s = specimen volume change during saturation
ε_a = axial strain
ε_r = radial strain
ε_v = volumetric strain
ϕ'_{cs} = critical state friction angle
ϕ'_{mob} = mobilized friction angle
V = Poisson's ratio
σ'_1 = effective major principal stress
σ'_3 = effective minor principal stress
A_o = initial cross sectional area of the specimen before consolidation
A_c = cross sectional area of the specimen after consolidation and before shear
A_e = effective area of specimen
B = Skempton's pore water pressure parameter
C_C = coefficient of curvature
C_U = coefficient of uniformity
G_S = specific gravity of soil particles
$D_{1/3}$ = average specimen diameter within the middle third portion of the specimen height
D_{50} = mean particle size
$D_{\max}$ = maximum specimen diameter
D_{rc} = consolidation relative density
D_c = specimen diameter after consolidation
D_s = nominal specimen diameter
e_c = consolidation void ratio
e_{critical} = specimen void ratio at the end of the test corresponding to a critical state
e_o = initial specimen void ratio
E_m = Young's modulus of the membrane material
H_o = initial specimen height
H_s = nominal specimen height
p', p'_c = mean consolidation stress
q = deviator stress measured in a triaxial shear test
S_r = specimen saturation ratio
$s_{u(\text{critical})}$ = undrained shear strength at the critical state
t_m = membrane thickness
u = pore water pressure
V_o = initial specimen volume

REFERENCES

Ansal, A.M. and Erken, A. (1996). "Posttesting correction procedure for membrane compliance effects on pore pressure." *Journal of Geotechnical Engineering*, **122**(1), 27–38.

ASTM Standard D2487 (2011). "Standard practice for classification of soils for engineering purposes (unified soil classification system)." *ASTM International*, West Conshohocken, PA, www.astm.org.

ASTM Standard D4253 (2006). "Standard test methods for maximum index density and unit weight of soils using a vibratory table." *ASTM International*, West Conshohocken, PA, www.astm.org.

ASTM Standard D4767 (2011). "Standard test method for consolidated undrained triaxial compression test for cohesive soils." *ASTM International*, West Conshohocken, PA, www.astm.org.

ASTM Standard D7181 (2011). "Standard test method for consolidated drained triaxial compression test for soils." *ASTM International*, West Conshohocken, PA, www.astm.org.

Baldi, G. and Nova, R. (1984). "Membrane penetration effects in triaxial testing." *Journal of Geotechnique*, **110**(3), 403–420.

Black, D.K. and Lee, L.L. (1973). "Saturating laboratory samples by back pressures." *Journal of Soil Mechanics and Foundation Engineering*, **99**(1), 75–93.

Bishop, A.W. and Green, G.E. (1965). "The influence of end restraint on the compression strength of a cohesionless soil." *Journal of Geotechnique*, **15**(3), 243–266.

Garga, V. and Zhang, H. (1997). "Volume changes in undrained triaxial tests on sands." *Canadian Geotechnical Journal*, **34**(3), 762–773.

La Rochelle, P., Leroueil, S., Trak, B., Blais-Leroux, L., and Tavenas, F. (1988). "Observational approach to membrane and area corrections in triaxial tests." *Advanced Triaxial Testing of Soil and Rock*, ASTM STP, **977**, 715–731.

Ladd, C.C. (1978). "Preparing test specimen using undercompaction." *Geotechnical Testing Journal*, **1**, 16–23.

Newland, P.L. and Allely, B.H. (1957). "Volume changes during drained triaxial tests on granular materials." *Journal of Geotechnique*, **7**, 17–34.

Nicholson, P.G., Seed, R.B., and Anwar, H.A. (1993). "Elimination of membrane compliance in undrained triaxial testing." *Canadian Geotechnical Journal*, **30**, 727–738.

Olson, R.R. and Campbell, L.M. (1964). "Discussion on importance of free ends in triaxial testing." *Journal of Soil Mechanics and Foundation Engineering*, **90**(6), 167–173.

Raju, V.S. and Sadasivan, S.K. (1974). "Membrane penetration in triaxial tests on sands." *Journal of Geotechnical Engineering*, **100**(4), 482–489.

Rowe, P.W. and Barden, L. (1964). "Importance of free ends in triaxial testing." *Journal of Soil Mechanics and Foundation Engi-*

neering, **90**(1), 1–27.

Russell, A.R. and Khalili, N. (2004). "Cavity expansion in unsaturated sands." *Proc., The 4th European Congress on Computational Methods in Applied Sciences and Engineering*, Jyvaskyla, 24–28.

Sarsby, R.W., Kalteziotis, N., and Haddad, E.H. (1980). "Bedding error in triaxial tests on granular media." *Journal of Geotechnique*, **30**(3), 302–309.

Sivathayalan, S. and Vaid, Y.P. (1998). "Truly undrained response of granular soils with no membrane-penetration effects." *Canadian Geotechnical Journal*, **35**, 730–739.

Ueng, T., Tzou, Y. and Lee, C. (1988). "The effect of end restraint on volume change and partical preakage of sands in triaxial tests." *Advanced Triaxial Testing of Soil and Rock*, ASTM STP, **977**, 679–691.

Zhang, H. (1997). "Steady state behavior of sands and limitations of the triaxial tests." Ph.D. dissertation, University of Ottawa, Canada.

Zhang, H. and Garga, V.K. (1997). "Quasi-steady state: A real behavior." *Canadian Geotechnical Journal*, **34**, 749–761.